Active/Reactive Power Control of PV Grid-tied NPC Inverter Using 3-D Space Vector Modulation in abc Coordinate

Dehghani Tafti, Hossein; Maswood, Ali Iftekhar; Roomi, Muhammad Musthafa

2015

Dehghani Tafti, H., Maswood, A. I., & Roomi, M. M. (2015). Active/Reactive Power Control of PV Grid-tied NPC Inverter Using 3-D Space Vector Modulation in abc Coordinate. 2015 IEEE Innovative Smart Grid Technologies - Asia (ISGT ASIA), 1-6.

https://hdl.handle.net/10356/82232

https://doi.org/10.1109/ISGT-Asia.2015.7387072

Active/Reactive Power Control of PV Grid-tied NPC Inverter Using 3-D Space Vector Modulation in abc Coordinate

Hossein Dehghani Tafti[1], *Student Member, IEEE*, Ali I. Maswood[2], *Senior Member, IEEE* and Muhammad M. Roomi, *Student Member, IEEE*.
School of Electrical and Electronic Engineering, Nanyang Technological University, Singapore
Email: [1]hossein002@e.ntu.edu.sg, [2]eamaswood@ntu.edu.sg

***Abstract*—Flexible active and reactive power injection to the grid is one of the requirements of medium-scale PV power plants (PVPP). Due to the high penetration of installed distributed generation (DG) units to the power system, the flexible active/reactive power control capability is necessary for medium-scale PVPPs in order to maintain the power quality and reliability of the power system. A three-dimensional space vector modulation (3-D SVM) in abc coordinate with combination of proportional-resonant (PR) controller is proposed for 4-wire NPC grid-connected inverter of the multi-string PVPP. The implementation of 3-D SVM in stationary coordinate (αβ coordinate) for 4-wire multilevel inverters requires high computational complexity. However, in the proposed 3-D SVM which is implemented in abc coordinate, the computational complexity is decreased and flexible balanced/unbalanced active/reactive power injection capability is achieved. The performance of the proposed controller is investigated on the three-level neutral-point-clamped (NPC) inverter of a 10 kW grid-connected multi-string PVPP, which is considered as the state of the art for medium-scale PVPPs. Various operation conditions like partial shading of PV strings and balanced/unbalanced grid faults are implemented.**

***Index Terms*—Photovoltaic systems, Active power control, Reactive power control, NPC inverter, 3-D Space Vector Modulation.**

I. Introduction

Photovoltaic energy has been in the focus of many governments and due to the considerable subsidies, experienced a rapid growth in the last few years. Due to the high penetration of installed photovoltaic power plants (PVPP) in the grid, new grid codes and standards are regulated in order to maintain the power quality and reliability of the power system. Consequently, PVPPs should be designed in order to inject the regulated active/reactive power to the grid during normal operation and also under grid faults [1], [2].

In order to enhance the power quality of the grid with unbalanced loads, medium-scale PVPPs should be able to inject unbalanced currents to three phases. Similarly under grid faults, medium-scale PVPPs should have the fault ride through (FRT) capability and inject required active/reactive power to the grid in order to enhance the point of common coupling (PCC) voltage and prevent the disconnection of protection breakers [3]-[5]. Several studies have considered injecting the balanced reactive current to three-phases even under unbalanced grid voltage sag condition. However, the probability of unbalanced voltage sags occurring is more common than balanced voltage sags. Unbalanced voltage sags result in negative sequence voltage and current in the grid [6], [7]. Consequently, the ability of the flexible active/reactive power injection is necessary for medium-scale PVPPs.

Two stage multi-string PVPPs consist of a DC/DC converter in each PV string and one central inverter and are popularly recognized as the state of the art for medium and high power PVPPs, due to their perceived advantages of higher energy conversion efficiency, modularity and power density. Multi-level converters have emerged as the most viable solutions for high power energy conversion due to their high power and capability of delivering excellent power quality with low harmonic contents, as well as achieving better efficiency as compared to the two-level converters. Therefore, the multi-string PVPP with multi-level converter is proposed for medium-scale PVPPs [8]. Due to the implementation of the single DC-link, the proposed PVPP extracts the maximum power from PV strings in all conditions. Besides, a proportional resonant (PR) controller in combination with the adaptive space vector modulation (ASVM) have been introduced.

In the previous study of authors [8], ASVM is implemented in stationary coordinate (αβ) which results in the increase of computational complexity. Additionally, three-dimensional space vector modulation (3-D SVM) should be implemented for 4-wire power systems. The implementation of 3-D SVM for multilevel inverters increases the computational complexity. However, the implementation of 3-D SVM in abc coordinate has several advantages like decreased computational complexity and better understanding of the switching states which can be useful for unbalanced current injection of the inverter as well the voltage balancing of DC-link capacitors [9], [10].

This paper proposes the 3-D SVM technique for neutral-point-clamped (NPC) inverter of medium-scale multi-string PVPP. The proposed 3-D SVM is implemented in abc coordinate. The input reference voltages of 3-D SVM are calculated with the proportional-resonant (PR) controller. The PR controller is implemented in αβ coordinate and its calculated reference voltages are transferred to abc coordinate using the inverse Clark transformation. Reference currents are calculated according to the extracted power from PV strings and PCC voltage. The proposed controller can inject unbalanced active/reactive power to the grid with the advantage of the implementation of 3-D SVM for generating the switching signals of NPC inverter. The performance of the proposed

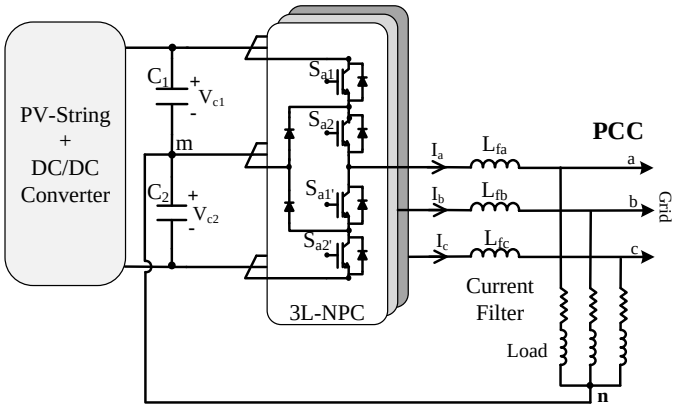

Fig. 1. Proposed Four-Wire Multi-string PV power plant

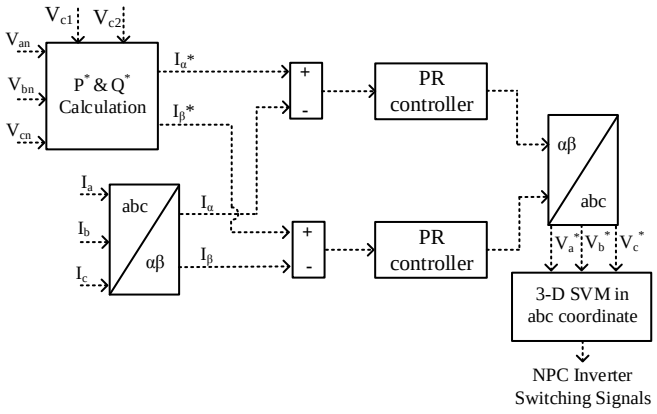

Fig. 2. Proposed VOC-PR Controller with 3-D SVM in abc coordinate

controller is investigated on a 10 kW multi-string PVPP under different operation conditions including partial shading of PV strings and balanced/unbalanced grid faults.

II. PVPP CONFIGURATION

A comprehensive structure of the proposed multi-string PV system with flexible active/reactive power injection capability depicted in Fig. 1 consists of PV strings, DC/DC converters and NPC inverter. The configuration of PV strings and DC/DC converters is presented in previous study of authors [8]. The grid-connected NPC inverter consists of two pairs of IGBT switches (S_{a1} and S_{a2}) including their complementary ($S_{a1'}$ and $S_{a2'}$) in each phase-leg. The NPC operates with three different switching states to synchronize the three output pole voltage stepped levels at $V_{dc}/2$, 0 and - $V_{dc}/2$ with respect to the midpoint of the DC-link (m). The neutral point of the load and grid are connected to the midpoint of the DC-link (m) in order to achieve the unbalanced current injection to PCC. This provides an additional advantage of improving power quality of the grid with unbalanced loads or under unbalanced voltage sags.

Filter inductors are connected in between the inverter and the grid to provide low current THD performance for the sake of complying with grid codes and IEEE standards [11]. The size of the filter inductors is calculated according to the following equation [12]:

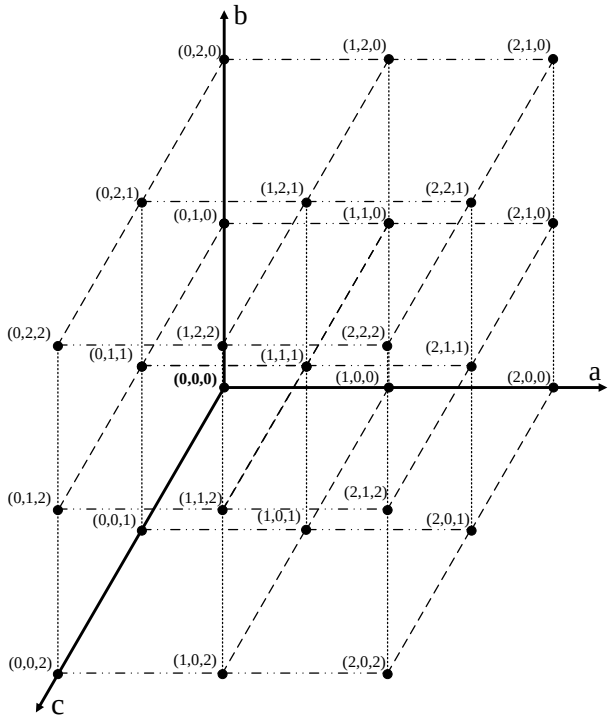

Fig. 3. 3-D space vector representation of the NPC inverter in abc coordinate

$$\Delta I_{L} = \frac{m_a V_{dc}}{2 L_f F_s}\left[m_a - \frac{1}{3} \right] \quad (1)$$

where:

L_f: Filter inductor (H)

m_a: Modulation index (The worst current ripple occurs at m_a=1, which considered to design the inductor.

F_s: Inverter switching frequency (Hz)

ΔI_L: Current ripple (A)

Maximum current ripple of 30% is considered to design the inductor.

III. PROPOSED CONTROLLER WITH 3D-SVM

The proposed voltage-oriented-control with PR controller (VOC-PR) in combination with 3-D SVM is depicted in Fig. 2. The reference stationary frame currents (I_α^* and I_β^*) are calculated based on the grid condition, PCC voltages (V_{an}, V_{bn} and V_{cn}) and DC-link capacitor voltages (V_{c1} and V_{c2}). During the grid normal operation, the inverter output power (P) is adjusted to the total extracted power from PV strings, while DC/DC converters are extracting maximum power from PV strings. After detecting the voltage sag by monitoring the grid voltage amplitude, the NPC controller should be changed in order to control its output reactive current according to the voltage sag level [13].

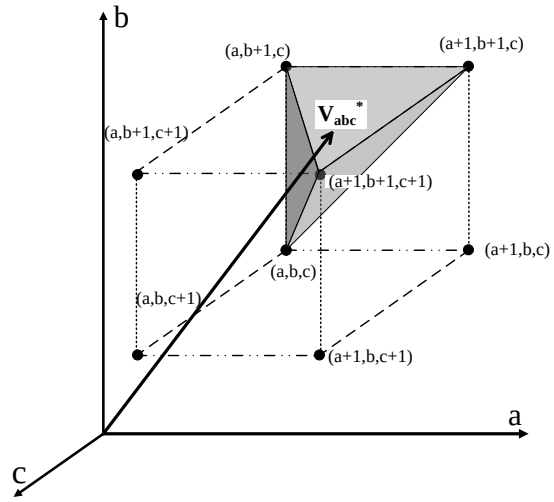

Fig. 4. Tetrahedron into the cube with corresponding state vectors of 3-D SVM

Subsequently, the respective α-β current errors are obtained by subtracting the reference stationary frame currents (I_α^* and I_β^*) with the stationary frame currents (I_α and I_β). Hence, the reference stationary frame voltages (V_α^* and V_β^*) are acquired from the proportional resonant (PR) controller and are fed into the 3-D SVM through the inverse Clark transformation. The PR controller is proven for its fast dynamic response and reduced steady state error. It can eliminate the steady state reference error by having its resonant frequency matching with the grid frequency [14].

3-D SVM representation of the NPC inverter is depicted in Fig. 3. In this figure, 0, 1, and 2 represent the different DC voltage levels which are connected to each phase of the converter, where 0 shows the lower DC voltage level ($-V_{dc}/2$), 1 indicates the connection between the neutral point and each phase and 2 is the connection of the higher DC voltage level and the corresponding phase ($+V_{dc}/2$). It can be easily seen that all possible switching states are considered in this diagram.

Since the switching of the converters stays as discrete states, 3-D SVM is considered to approximate the reference voltages (V_a^*, V_b^* and V_c^*). The space vector representation of the NPC inverter consists of eight cubes as shown in Fig. 4. Flow chart of the 3-D SVM is represented in Fig. 5. First, the integer part of input reference voltages are calculated to indicate the corresponding cube according to below:

$$\begin{cases} \text{if } V_a^* < 0 & a = 0 \\ \text{if } V_a^* \geq 0 & a = 1 \end{cases} \quad (2)$$

where a indicates the integer value of reference voltages of phase A. Similarly, the integer values of voltages of phase B and C are also calculated. These integer values show the corresponding cube of Fig. 3 which the reference voltage vector is located.

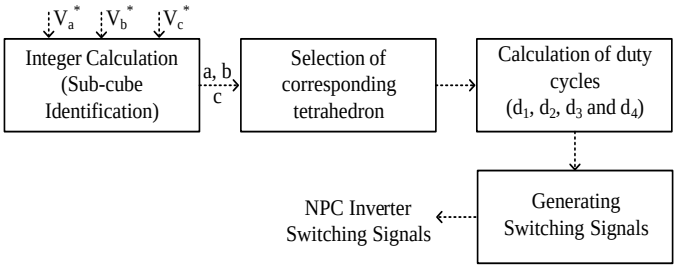

Fig. 5. Flowchart of 3-D SVM for NPC inverter

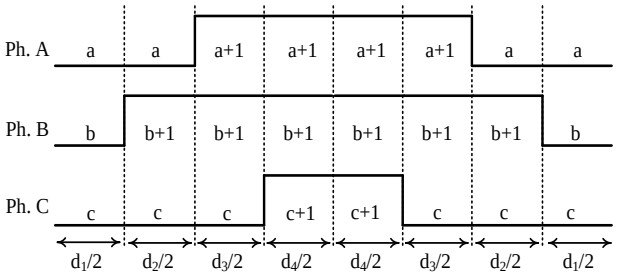

Fig. 6. Switching states of 3-D SVM for NPC inverter

Since six tetrahedrons are considered in each cube, it is required to identify the tetrahedron where the reference voltage vector is locating. This tetrahedron is easily found using comparisons with the three planes in the 3-D space which define the six tetrahedrons inside the cube. The detailed comparison is presented in [9]. Once (a, b, c) coordinates are identified, the main step of the algorithm includes of calculating the four space vectors corresponding to the four vertices of a tetrahedron in the selected cube. These vectors will generate the reference vector. Finally, the switching time (duty cycle) of each switching state is calculated.

Switching states of one cycle of the reference which is considered in Fig. 4 are represented in Fig. 6. The symmetric switching state is selected in this study in order to minimize the switching variations of switches and reduce the switching frequency. It can be seen that 3-D SVM can be easily implemented for 4-wire NPC inverter in abc coordinate. Additionally the relevant switching states are directly related to the reference voltage and consequently unbalanced output currents can be easily achieved by considering the unbalanced references.

IV. Evaluation Results

The performance of the proposed controller with 3-D SVM is investigated on the 10 kW multi-string PVPP (Fig. 1), which is modelled and developed in Matlab/Simulink© and PSIM software. The PV panels are modelled according to the SHARP NU-U235F1 specifications (maximum power of 235 W with voltage of 30 V and currents of 7.84 A, under 25°C temperature and 1 kW/m^2 irradiance). Two PV strings are considered in the PVPP which are connected to the DC-bus through a DC/DC boost converter. Based on the grid voltage (V_L=400 V_{rms}), the

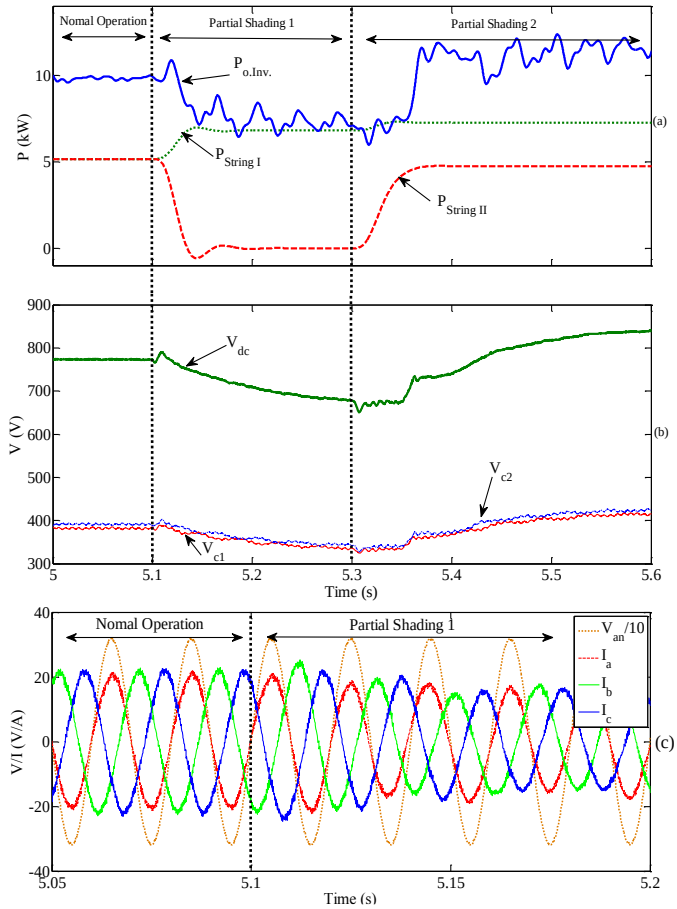

Fig. 7. Dynamic performance of the PV grid connected inverter under various temperature and irradiation conditions: (a) PV string power and inverter output power, (b) DC-link and capacitor voltages and (c) Grid currents and phase voltage.

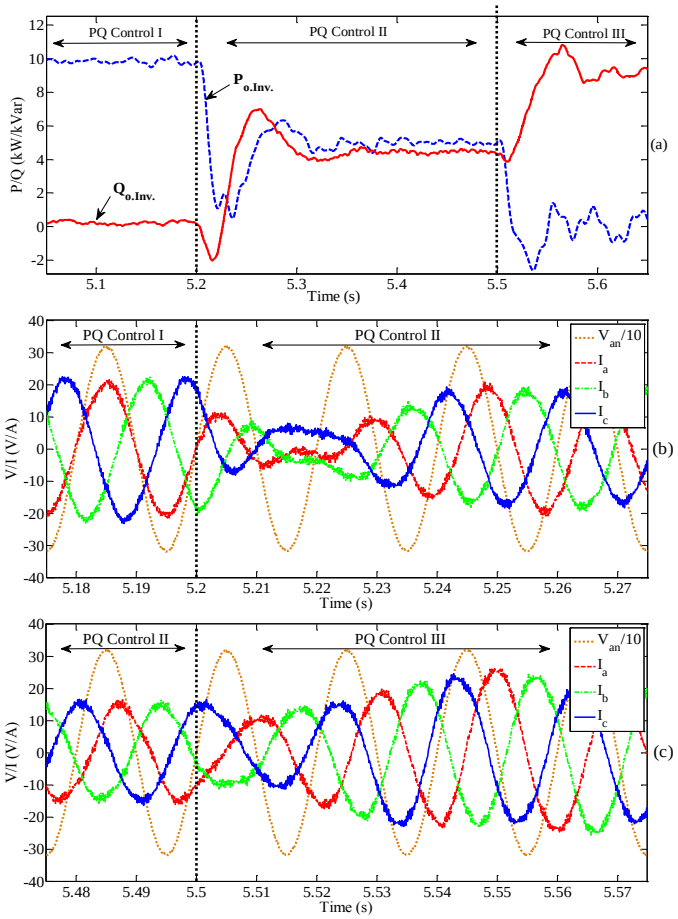

Fig. 8. Performance of the proposed controller under different balanced PQ control strategies: (a) Inverter active and reactive power, (b) Inverter current and PCC phase voltage under PQ control I and II, and (c) Inverter current and PCC phase voltage under PQ control II and III.

DC-bus voltage (V_{dc}) is 770 V. Consequently 22 PV panels are connected in each PV-string to create voltage of 660 V in each string [8]. The detailed setting of the simulated system is presented in Table I.

The dynamic performance of the proposed controller under the normal grid operation is evaluated in Fig. 7 under the three different conditions listed in Table II. The proposed system is operated initially with the three PV string modules having the same parameters between t=0 s to t=5.1 s. During the second condition (from t=5.1 s onwards), different amounts of irradiance is experienced by String I (irradiance increase: Irrad=1.4 kW/m^2) and String II (complete shading: Irrad=0 kW/m^2). The irradiance in String II is recovered to 0.9 kW/m^2 while there is a decrease in the temperature strings during t=5.3 s to t=5.6 s.

As shown in Fig. 7(a) under the normal operation (before t=5.1 s), all PV strings are receiving Irrad=1 kW/m^2 and the boost converter of each PV string extracts the maximum power from that PV string (P_{String}=5 kW). String II experiences a complete shading at t=5.1 s and accordingly $P_{String\ II}$ is reduced to zero. The extracted power of String I ($P_{String\ I}$) is growth due to the increment of its irradiance. During this period, the

TABLE I. SIMULATION PARAMETERS

Parameter	Symbol	Value
Grid Voltage	$V_{PCC\text{-}ab}$	400 $V_{l\text{-}l,rms}$
Grid Frequency	f	50 Hz
Line Inductor	L_f	7.5 mH
DC-link Capacitor	C_1 , C_2	2.475 mF
DC-link Voltage	V_{dc}	770 V_{dc}
NPC Switching Frequency	$f_{s,inv.}$	7.2 kHz

TABLE II. DYNAMIC OPERATING CONDITIONS OF PV STRINGS

Time (s)	String I	String II
0 – 5.1 (Normal Operation)	Irrad = 1* Temp = 25*	Irrad = 1 Temp = 25
5.1 – 5.3 (Partial Shading 1)	Irrad = 1.4 Temp = 25	Irrad = 0 Temp = 25
5.3 – 5.6 (Partial Shading 20	Irrad = 1.4 Temp = 20	Irrad = 0.9 Temp = 20

* Irrad and Temp are referred to the individual irradiance (kW/m^2) and temperature (°C) respectively.

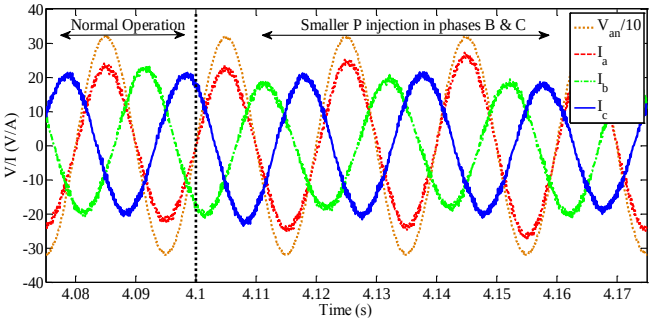

Fig. 9. Inverter output current under unbalanced active power injection

proposed VOC-PR controls the output inverter power according to the $P_{st.Total}$ by reducing the amount of the injected current to the grid and as a result the output power of the grid-connected NPC inverter is also reduced as depicted in Fig. 7(a). The DC-link voltage is maintained to its nominal range during all conditions as depicted in Fig. 7(b). It can be observed that there is a decrease in the magnitude of the three-phase grid currents in Fig. 7(c) due to the reduction of the inverter output power. The irradiance of Sting II is recovered to 1.4 kW/m^2 at t=5.3 s and consequently the $P_{String\ II}$ and $P_{O.Inv}$ are raised.

The unity power factor operation is maintained throughout all environmental conditions as shown in Fig. 7 (c). Additionally despite of such extreme shading conditions, there are no voltage and current spikes experienced at the ac grid side with the implementation of the proposed VOC-PR control scheme.

The performance of the proposed controller is investigated under three different balanced active/reactive control strategies as below in Fig. 8:

- PQ Control I: P*=Smax, Q*=0,
- PQ Control II: P*=Smax/2, Q*= Smax/2,
- PQ Control III: P*=0, Q*= Smax.

where S_{max} is the maximum apparent power of the inverter. It should be mentioned that under partial shading conditions, S_{max} is calculated based on the total extracted power from all PV strings.

As shown in Fig. 8(a), before t=5.2 s, the inverter only injects active power to the grid while its reactive power is zero. Consequently, there is no phase shift between the inverter current and PCC phase voltages as depicted in Fig. 8(a) and the inverter is operating under unity power factor. The controller is modified to inject both active and reactive powers during t=5.2 s and t=5.5s. Accordingly, there is a phase shift between phase voltage and current of the inverter during this interval. The phase shift is smaller than π/2 rad as depicted in Fig. 8(b). The controller strategy is changed to inject only reactive power after t=5.5 s. Consequently, the inverter active power is decreased to zero and phase difference between inverter current and PCC voltage is π/2 rad as shown in Fig. 8(c).

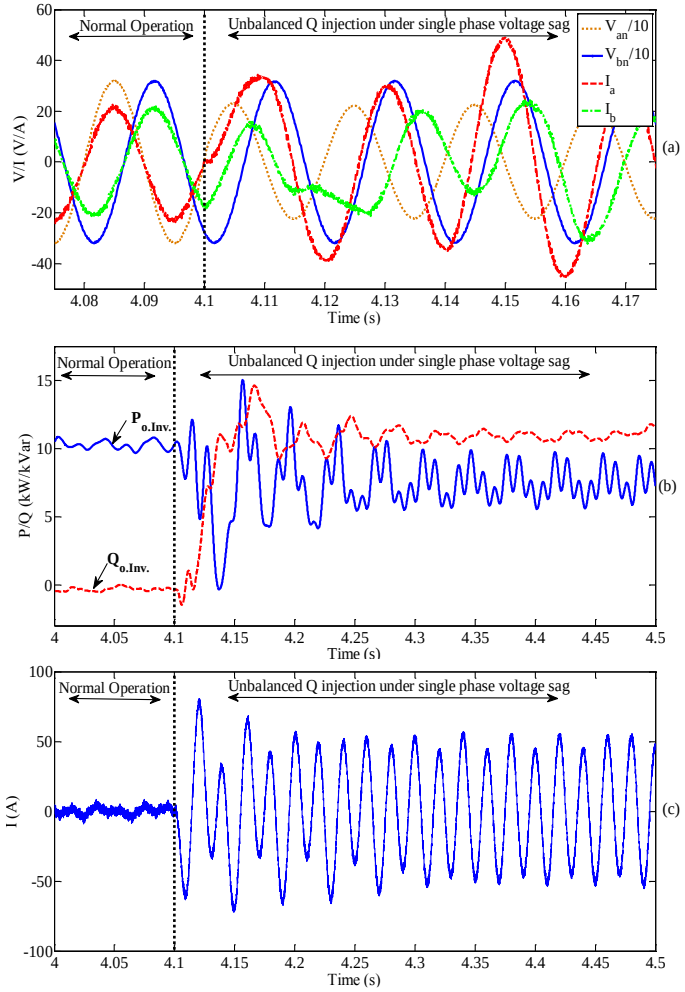

Fig. 10. Performance of the proposed controller under single phase fault: (a) PCC voltage and phase current and (b) Injected active/reactive power, (c) Neutral wire current

The performance of the proposed controller is investigated under unbalanced active power injection in Fig. 9. Before t=4.1 s, the inverter in injecting balanced active power to all three phases under normal grid operation and it can be obsereved that there is no phase shift between phase current and voltages. At t=4.1 s, the controller is modfied to inject 80% of its nominal active power to phases B and C and inject 120% of its nominal power to phase A. It can be obsereved that I_b and I_c are reduced while I_a is increased following the refrence currents. On top of that, the inverter is operating under unity power factor for all phases even under unbalanced active power injection and because of fast response opertion of the PR controller, there is no spikes in the current of the inverter.

Fig. 10 depicts the performance of the proposed controller under single-phase grid fault of phase A. It can be observed that after t=4.1 s, the voltage of phase A is decreased to 75% of its nominal value. Consequently, the inverter injects reactive power to the grid according to grid codes and there is approximately π/2 rad phase difference between current and voltage of each phase. Additionally the injected current and reactive power to phase A is higher than the current of other phases in order to

enhance the voltage of this phase. The injected active and reactive power under single phase fault is depicted in Fig. 10(b). It can be observed that after occurance of single pahse fault, the injeected active is reduced and accordingly the injected reactive power is increased. It should be mentioned that due to the unbalanced injection of active and reactive power to the grid during this unbalanced grid fault, the amount of active/reactive power experienced some ripples. On top of that, as depicted in Fig. 10 (c) due to the unbalanced current injection, the curent of neutral wire does not remain zero. However, due to the implentation of 3-D SVM, the voltage of DC-link capacitors remains balanced.

Thus, the evaluation results have evidently proven that excellent flexible active/reactive power injection capability is achieved for the proposed multi-string PV plant in Fig. 1 under both normal operation and balanced/unbalanced grid fault conditions. The proposed controller allows the PV power plant to stay connected to the grid and inject required unbalanced currents to the grid in order to enhance the PCC voltages under faults and avoid the disconnection of protection breakers.

V. Conclusion

This paper proposes the 3-D SVM in abc coordinate in conjunction with voltage oriented control using the proportional-resonant controller (VOC-PR) for grid-connected medium-scale multi-string PVPP with NPC inverter which is connected to 4-wire power system. The implementation of the 3-D SVM in abc coordinate decreases the computational complexity as compared to the implementation of this technique in stationary frame. Besides, the current of the inverter is controlled through the PR controller which eliminates the multiple frame transformation compared to the conventional PI controller. A flexible active/reactive power control is achieved with the proposed controller. Moreover, the PVPP can stay connected to the grid under grid faults and inject required unbalanced reactive power to the grid in order to enhance the PCC voltages. As a reason of the elimination of multiple frame transformation, the proposed controller shows faster dynamic response and smaller steady state error as compared to the conventional PI controller. The evaluation results have proven the applicability of the proposed controller for medium-scale PVPPs in order to comply with new grid codes and standards and maintain grid power quality in different operation conditions.

VI. References

[1] Hoffmann, A.; Fleckenstein, M.; Balzer, G.; Hartkopf, T., "Grid services with PV-converters in distribution systems," *in Innovative Smart Grid Technologies Conference (ISGT), 2014 IEEE PES*, pp.1-5.

[2] N. Saadat, S. S. Choi, and D. M. Vilathgamuwa, "A series-connected photovoltaic distributed generator capable of enhancing power quality," *IEEE Trans. Energy Convers.*, vol. 28, no. 4, pp. 1026–1035, 2013.

[3] Characteritics of the utility interface forphotovoltaic (PV) systems, IEC Std. 61727-2002.

[4] Grid Code - High and Extera High Voltage, Bayreuth, Germany: E. On GmbH, 2006.

[5] B. I. Craciun, T. Kerekes, D. Sera, and R. Teodorescu, "Overview of recent Grid Codes for PV power integration," in Optimization of Electrical and Electronic Equipment (OPTIM), 2012 13th International Conference on, 2012, pp. 959-965.

[6] A. Camacho, M. Castilla, j. miret, R. Guzman, and A. Borrell, "Reactive Power Control for Distributed Generation Power Plants to Comply With Voltage Limits During Grid Faults," *Power Electronics, IEEE Transactions on*, vol. 29, pp. 6224-6234, 2014.

[7] A. Camacho, M. Castilla, J. Miret, A. Borrell, and L. Garcia de Vicuna, "Active and Reactive Power Strategies With Peak Current Limitation for Distributed Generation Inverters During Unbalanced Grid Faults," *Industrial Electronics, IEEE Transactions on*, vol. 62, pp. 1515-1525, 2015.

[8] H. Dehghani Tafti, A. I. Maswood, A. Ukil, O. H. P. Gabriel, and L. Ziyou, "NPC photovoltaic grid-connected inverter using proportional-resonant controller," in *Power and Energy Engineering Conference (APPEEC), 2014 IEEE PES Asia-Pacific*, 2014, pp. 1-6.

[9] M. Prats and L. Franquelo, "A 3-D space vector modulation generalized algorithm for multilevel converters," *IEEE Power Electron. Lett.*, vol. 1, no. 4, pp. 110–114, 2003.

[10] L. G. Franquelo, M. Á. M. Prats, R. C. Portillo, J. I. L. Galvan, M. a. Perales, J. M. Carrasco, E. G. Díez, and J. L. M. Jiménez, "Three-dimensional space-vector modulation algorithm for four-leg multilevel converters using abc coordinates," *IEEE Trans. Ind. Electron.*, vol. 53, no. 2, pp. 458–466, 2006.

[11] "IEEE standard for interconnecting distributed resources with electric power systems," IEEE Std 1547-2003, July 2003.

[12] H. Ooi, A. Maswood, and Z. Lim, "Five-Level Multiple-Pole PWM AC-AC Converters with Reduced Components Count," *Industrial Electronics, IEEE Transactions on*, vol. PP, pp. 1-1, 2015.

[13] Dehghani Tafti, H.; Maswood, A.I.; Lim, Z.; Ooi, G.H.P.; Raj, P.H., "NPC photovoltaic grid-connected inverter with ride-through capability under grid faults," in *Power Electronics and Drive Systems (PEDS)*, 2015 *IEEE 11th International Conference on*, pp.518-523.

[14] R. Teodorescu, F. Blaabjerg, M. Liserre, and P. Loh, "Proportional resonant controllers and filters for grid-connected voltage-source converters, "Electric Power Applications, IEE Proceedings, vol. 153, no. 5, pp.750–762, September 2006.